Reduction of Ice Adhesion on Nanostructured and Nanoscale Slippery Surfaces

Luke Haworth[a], Deyu Yang[b], Prashant Agrawal[a], Hamdi Torun[a], Xianghui Hou[b], Glen McHale[c], Yongqing Fu[a,*]

[a] Faculty of Engineering and Environment, University of Northumbria, Newcastle Upon Tyne, NE1 8ST, U.K

[b] State Key Laboratory of Solidification Processing, Shaanxi Key Laboratory of Fiber Reinforced Light Composite Materials, Northwestern Polytechnical University, Xi'an 7100 72, China

[c] Institute for Multiscale Thermofluids, School of Engineering, The University of Edinburgh, Kings Building, Edinburgh, EH9 3FB, U.K.

[*] Corresponding author: Prof. Richard Yongqing Fu, email: richard.fu@northumbria.ac.uk

Abstract

Ice nucleation and accretion on structural surfaces are a source of major concerns for safety and operations in many industries such as aviation and renewable energy sectors. Common approaches to tackle these involve the uses of active methods such as heating, ultrasonic or chemical methods, or passive methods such as surface coatings. In this study, we explored the ice adhesion properties of slippery coated substrates by measuring shear forces which were required to remove a glaze ice block on the coated substrates. Among the studied nanostructured and nanoscale surfaces (e.g., a superhydrophobic coating, a fluoro-polymer coating, and a PDMS chain coating), the PDMS chain coated surface, with its flexible polymer brushes and liquid-like structure, significantly reduced the ice adhesion on both glass and silicon surfaces. Further studies on the PDMS chain coating on the roughened substrates also demonstrated its low ice adhesion. The reduction in ice adhesion is attributed to the flexible nature of brush-like structures of PDMS chains, allowing ice to be easily detached.

Keywords: Hydrophobic, superhydrophobic, polymer surface, ice adhesion, wettability, SOCAL

Article Highlights:

- Introduces several simple and reproducible techniques to significantly reduce ice adhesion on surfaces based one surface coatings and identifies the coating with the lowest adhesion.
- Explores the lowest adhesion coating on surfaces with micro and macro structures and find a continued reduction in ice adhesion.
- Explores qualitatively and quantitatively through surface morphology and an analytical model the results of the ice adhesion values obtained giving justification for all results obtained.

Ice accretion and adhesion have damaging impacts on many sectors, including but not limited to aviation, renewable energy, and telecommunications [1-4]. For example, ice formation on aircraft wings poses a great hazard to health and safety. According to the Aircraft Owners & Pilots Association (AOPA) Air Safety Foundation, between 1990 and 2000, there were 105 accidents involving fatalities due to the effects of icing [5]. Renewable energy generation is a key growing area to reduce the amount of energy generated from fossil fuels, but when considering the impact that cold weather can have on wind turbines, ice formation can result in power loss, mechanical and electrical failure and safety issues [6]. Common passive approaches to tackle this issue have either involved simple painting of the surface or more complex icephobic treatments [7-9]. Extensive studies have been attempted in the field of icephobic coatings for passive prevention of ice accretion and reduction of ice adhesion on the surface. The most simple type of passive coating is black colour substances to allow for solar heating [10]. However, there may not be sufficient sunlight especially during dark winter days or periods of heavy rainfall.

Recently the focus of fabricating new icephobic coatings has been centred around nature-inspired coatings. Superhydrophobic surfaces (SHS) based on nanoscale features on microscale structures have been explored for achieving icephobicity [7-9]. These surfaces are highly water repellent and have large contact angles. However, their problems include mechanical durability over time as the coating easily breaks down through repeated testing, and potential nucleation sites due to their microporous structures which can result in condensate freezing. Various polymer coatings have also been explored in terms of their anti-icing capabilities. Such surfaces are promising for applicability to a wider range of surfaces and for a longer-term use. For example, Kreder et al [11] summarized that various polymer coatings can be used (combining SHS with nanostructures) to lower the ice adhesion. Fluorinated polymer-based coatings have also been shown to achieve a low ice adhesion (of the order of 10 kPa) [12-14], and they were fabricated from polytetrafluoroethylene (PTFE) or polydimethylsiloxane (PDMS) elastomers which have been cross-

linked with other varied fluorinated polymer surfaces, such as fluorinated polyhedral oligomeric silsequioxane (POSS). The influence of PDMS based surfaces for low ice adhesion has also been investigated including the use of PDMS surfaces from methylated and non-methylated surfaces, lubricant infused PDMS brush structures and cross-linked PDMS structures, PDMS-loop structures of varying chain lengths and PDMS brushes imbibed with toluene vapour [15-18]. These investigations on the ice adhesion strength of variations of polymer coatings reported ice adhesion values ranging from 0.55-100 kPa depending on the surfaces under investigation and slippery nature of the PDMS coatings.

Previously mentioned studies on superhydrophobic coatings often suggest that the smoother the surface, the better the performance due to the increased difficulty in ice nucleation. Whilst previous studies on polymer coatings have largely been focused on altering the surfaces and coating chemistry, there have been minimal studies which investigate the influences of altering a substrates physical properties before coating with such polymer coatings with respect to ice adhesion. For applications in industry, the ability to reduce ice adhesion on a rough or roughened surfaces of components is critical.

In this study, we compare two different nanoscale hydrophobic polymer surfaces against a porous superhydrophobic coating on both glass and silicon substrates. The first polymer coating is an amorphous fluoropolymer with relatively solid/rigid but randomly orientated nanostructures. The second one consists of a flexible and slippery nanoscale coating formed from PDMS chains. Both polymer coatings covalently bond with the surface of glass and silicon and have similar chain lengths but different physical properties. Additionally, the silicon substrates were physically altered to produce roughness in different scales to study their influences on ice adhesion. We compared the ice adhesion values of all surfaces, both glass and silicon, smooth and roughened, to those from an analytical model which empirically estimates the ice adhesion based on the receding contact angle of water on the different surfaces. We finally verified that after repeated ice adhesion testing, the surfaces have not been significantly changed in terms of their wettability and therefore they have some robustness in terms of stability in wettability.

The substrates used in this study include cover glass slips (~170 μm thickness) and silicon wafers (500 μm thickness). They were thoroughly cleaned before the surface treatments. The three surface treatment methods for these substrates include: 1) hydrophobic nanoparticles (Glaco Mirror coat Nippon Shine), , 2) polymer treatment using amorphous fluoro chains (CYTOP AGC Chemicals Company), and 3) a

PDMS chain structure (a so-called slippery omni-phobic covalently attached liquid (SOCAL) surface). The Glaco coated surface represents a porous superhydrophobic nanoparticle surface. The CYTOP represents a rigid but randomly orientated polymer chain structure. The PDMS chain structures have previously been reported as having flexible vertical arrangement which gives rise to a 4.7 nm thick brush-like and liquid-like solid coating [19].

To prepare the surfaces, the substrates first underwent a standard cleaning process consisting of sonication in a cleaning fluid solution (Decon 90) with deionised (DI) water followed by further sonication in DI water. The substrates were then cleaned with solvents consisting of acetone, followed by isopropanol (IPA) and finally rinsed in DI water and dried with compressed air. Following the cleaning procedure, the Glaco surface [20], containing hydrophobic silica nanoparticles (~100 nm diameter) suspended in IPA were deposited on the various substrates. The IPA was then allowed to evaporate leaving the particles on the structure and this was repeated 5 times. The result was a superhydrophobic nanoporous structure of approximately 1.7 μm thickness [20].

The next surface treatment involved depositing a thin layer of an amorphous fluoropolymer solution (CYTOP) onto pre-cleaned substrates via a dip coating method to ensure an even coating across the substrate. Following dipping, the sample was then placed in a tube furnace at 150 °C for 25 minutes. Subsequent to curing, the obtained substrate surface was covalently bonded with the fluoropolymer chains.

The SOCAL surface was fabricated through the acid catalysed polycondensation of dimethyldimethoxysilane (DMDEOS), whereby the DMDEOS was mixed with 98 % concentration of sulfuric acid in a solution of IPA to create a liquid-like hydrophobic surface [19]. Once the samples were cleaned, they were treated in the plasma oven for 30 minutes at a power of 30 W to create OH^- radicals on the surface. Following this step, the samples were immersed in the solution for 5 s before a slow manual withdrawal from the solution and curing in a humidity chamber at 65% relative humidity (for 20 minutes). This process allowed for the solution to react with the exposed radicals on the surface, inducing the polycondensation of the PDMS chains on the surface and creating the polymer chain structure, which results in low surface energy and low contact angle hysteresis [21].

To form the different roughed surfaces, silicon wafers were chosen as the substrates. Two different grades of sandpaper were used to generate different surface roughness values. The sandpaper was rubbed repeatedly over the sample for approximately 5 minutes, using a fabricated block to ensure that the sandpaper was remained in contact with the surface and with a sufficient pressure. The first grade of sandpaper chosen was P120, this was classed as a macro grit sandpaper with grit diameter of 162 μm and from this point onwards, and the samples that were roughened using this grit will be referred to as Si P120 samples. The second grade of sandpaper chosen was P1200 which was a micro grit sandpaper and had a grit diameter of 23 μm, and from this point onwards, the samples that were roughened using this grit will be referred to as Si P1200 samples.

To characterise the wettability of the surface coatings, contact angles (advancing, θ_{adv} and receding, θ_{rec}) and the contact angle hysteresis ($\Delta\theta$) of the various surfaces were measured using a Drop Shape Analyser (Kruss DSA-30). The contact angles for the untreated, Glaco and CYTOP surfaces were measured using an inflation-deflation procedure where 4 μL DI water droplets were deposited on the surface before inflation and deflation of 2 μL at a flow rate of 0.5 μL/s. For the SOCAL surface, 4 μL DI water droplets were deposited on the surface before inflation by 2 μL at a flow rate of 0.033 μL/s for 60 s and then a slow evaporation at room conditions (~ 24 °C and ~ 40 % RH).

For the Glaco surface, the coating thickness is of the scale of 1 μm despite being a collection of nanoparticles and therefore a scanning electron microscopy (SEM) image was taken. However, for the two types of nanometric polymer coatings, this method is not suitable and therefore an atomic force microscope (AFM) was used. To characterise the surface roughness of the Glaco coating and sanded samples, the roughness was measured using an optical profilometer (Bruker ContourGT) within a surface area of 1.7 x 2.5 mm^2.

The ice adhesion tests were carried out using a horizontal shear force ice adhesion tester [22]. Silicone moulds were filled with DI water and placed on different substrates and coatings. The samples were placed in a cold chamber for three hours for the water to be frozen on the substrate. Once the samples were frozen, they were placed in the ice adhesion testing set-up and the force required to remove the ice block was recorded.

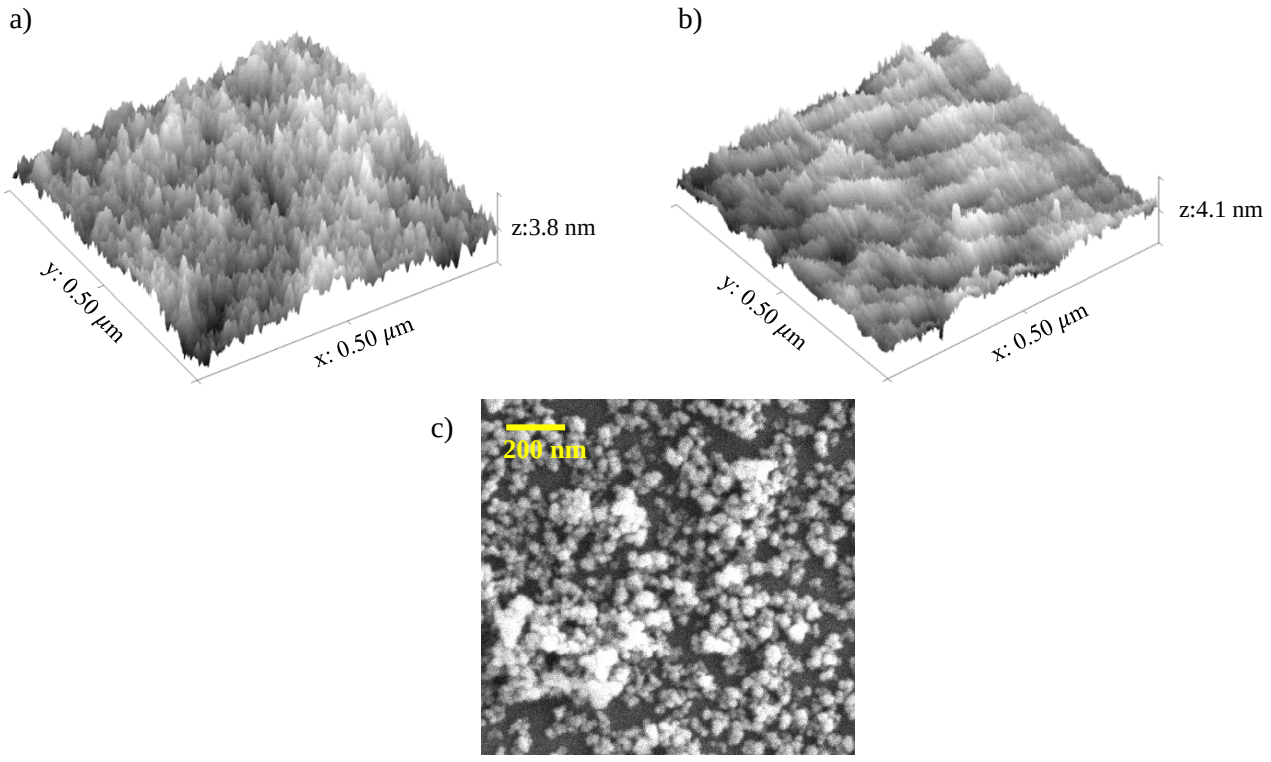

Figure 1a) 3D AFM image of CYTOP surface. b) 3D AFM image of SOCAL surface. c) SEM image of Glaco surface.

Figures 1a and 1b show the obtained 3D profile AFM images for the CYTOP and SOCAL surfaces. Figure 1c shows an SEM image taken over a 1 μm scan at 6.0 kV to illustrate the micro scale Glaco coating consisting of hydrophobic nanoparticles. From the AFM image for CYTOP, the root-mean-squared (RMS) roughness is 0.40 nm with an average maximum height of 2.17 nm. The random structure of the CYTOP coating can be assumed due to no clear regular patterns as shown in Figure 1a. The SOCAL structure on the other hand has an RMS roughness of 0.75 nm with an average maximum height of 14 nm. Figure 1b illustrates that there is more of an order to the polymer chains as seen by the distinct vertical ridges which might indicate an ordered vertical alignment. The SEM image of Glaco clearly illustrates the porous nature, where in some cases there are very few particles, and the silicon substrate underneath is visible. Figure 1c also illustrates the formation of clumps of nanoparticles and this microstructure created from the hydrophobic nanoparticles gives rise to the superhydrophobicity.

Table 1 lists the obtained root-mean-squared (RMS) roughness values for the untreated glass, Glaco and silicon samples, both untreated and roughened ones. The CYTOP and SOCAL values are mentioned above from the AFM results. From the data listed in the table, the Si P120 surface has the highest RMS roughness which is to be expected as it is generated with sandpaper that has a much higher roughness value. The Si P1200 sample has lower RMS roughness, which is generated using sandpaper with a much finer scale roughness. In both cases, the addition of the PDMS chains in SOCAL appears to make the surface slightly smoother.

Table 1. Roughness measurements for the surfaces in this study

Surface	Root-mean-squared (RMS) Roughness (μm)
Glass Untreated	0.005 ± 0.002
Glass Glaco	0.07 ± 0.00
Si Untreated	0.0003 ± 0.0001
Si SOCAL	0.00075 ± 0.0001
Si P120 Untreated	0.19 ± 0.07
Si P120 SOCAL	0.12 ± 0.01
Si P1200 Untreated	0.16 ± 0.03
Si P1200 SOCAL	0.14 ± 0.02

Figure 2a illustrates the differences in contact angle measurements (θ_{adv} for advancing contact angle and θ_{rec} for receding contact angle) on the cover glass substrates before and after the repeated ice adhesion testing, and Figure 2b shows the contact angle hysteresis ($\Delta\theta$, difference between θ_{adv} and θ_{rec}). For the ice adhesion results after testing, each surface underwent 15 ice adhesion tests before the contact angle values were measured again to investigate the changes. All values in Figure 2 are the average ones for 7 repeats on 3 different samples, therefore the standard deviation values were obtained. Ice adhesion results

were obtained from 5 measurements. For the untreated glass surface, the contact angles don't appear to change significantly, however the hysteresis is decreased. This may be due to surface damage due to ice adhesion testing. For the coated glass surfaces before the adhesion testing, the contact angle data match closely with those reported in literature for the Glaco and SOCAL surfaces [20, 21]. For the CYTOP surface before testing, the values obtained match closely with the manufacturer's reported values. Following adhesion testing on glass samples, there are minimal changes in θ_{adv}, θ_{rec} and $\Delta\theta$ which shows that the coating wettability has not been significantly changed due to surface damage during testing. For the roughened silicon samples, whilst the surface roughness is decreased by adding the SOCAL, θ_{rec} is increased and $\Delta\theta$ is changed. This indicates that the morphology of the SOCAL surface is slightly different and therefore the mobility of the contact line of a droplet on the surface has been changed. This change in contact line mobility and change in receding angle could cause increased ice adhesion. Similarly, contact angle hysteresis has increased following ice adhesion testing in almost all cases. This may be because following repeated ice removal, the nanoscale surface structure has been disrupted by adding more scratches on the nanometric scale. However, the contact angle data shows that the wettability of the substrate is not significantly affected in the case of the SOCAL.

As the untreated glass surface is hydrophilic, a droplet on it preferentially wets the surface. Whereas for the various coatings on cover glass, the roughest surface is Glaco. This is mainly due to the porous nature of the coating formed of nanoparticles with 100 nm diameter. This porosity is also the characteristic of the superhydrophobic properties of the coating. As previously shown in the experimental results, the CYTOP coating has a lower RMS roughness than the SOCAL. However, there is a larger hysteresis, which is due to the nature of the CYTOP. The random orientation of the polymer chains results in a surface which has a more variable morphology and therefore when a droplet is undergoing the inflation and deflation, there may not be a smooth change and so a larger value of hysteresis. For the SOCAL coating, whilst there is a higher RMS roughness, there is a more orientated pattern, whereby more chains are vertical as shown by the distinct lines in the AFM image. SOCAL has been shown to behave as a liquid, due to the flexible nature of the PDMS chains [15]. Therefore, as the droplet is inflated there is a smoother movement of the contact line leading to a lower hysteresis.

When considering the silicon samples, the untreated silicon sample is atomically smooth. However, due to its intrinsic chemical nature, a water droplet wets the surface and therefore the contact angle is lower than that of the SOCAL surface. When the samples are roughened, there is a significant disruption to the surface in the form of increased roughness. As a result, a droplet wets the surface further and has an even lower contact angle. Due to the morphology of the SOCAL coating, there is a lowered RMS roughness compared with a surface devoid of treatment. As the PDMS chains in SOCAL are flexible and nanoscale, they follow the pattern of the microstructure. Therefore, despite the addition of the nanoscale liquid-like coating, the droplet encounters an overall rough surface. This change in the surface morphology due to the roughness affects the movement of a droplet across the surface by increasing the receding angle and the hysteresis.

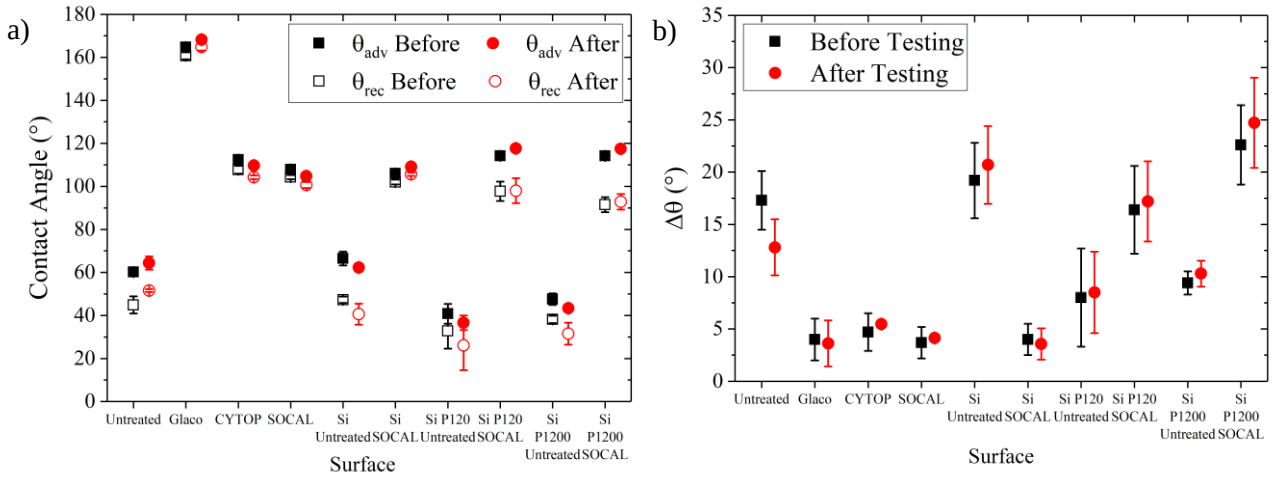

Figure 2a) Contact angle values before and after ice adhesion testing. b) Contact angle hysteresis before and after testing for all surfaces.

When investigating the ice adhesion strength on surfaces, an analytical equation was applied in which the shear ice adhesion strength is proportional to practical work of adhesion [15],

$$W_p = A\gamma_w(1 + \cos\theta_{rec}), \quad [1]$$

where A is a proportionality constant, γ_w is the surface tension of a water droplet with air, and θ_{rec} is the receding contact angle. Using equation 1 and the receding contact angle data from Figure 2a, the ice adhesion strengths for a droplet of DI water on untreated cover glass, Glaco, CYTOP and SOCAL surface were obtained, which are 22.87, 0.81, 10.02 and 10.08 kPa, respectively. Given that CYTOP and the SOCAL surfaces have similar receding contact angles, their analytical values are similar. Based on

Equation 1 and the data in Figure 2, the untreated surface has the highest analytical value and that Glaco surface has the lowest analytical value.

Figure 3 illustrates the differences in the ice adhesion strength results on the cover-slip glass among the different coatings and the untreated sample. For each surface, 4 repeats were carried out. In the case of SOCAL due to the scale and the small standard deviation of repeats, these appear as one point. It should be noted that the experimental values for untreated, Glaco and CYTOP lie relatively close to the analytical data (see the different lines in Figure 3). The Glaco surface reduces the contact area of a droplet with the surface with a superhydrophobic nature. This reduction in contact area is linked with the high receding and advancing angles which helps to significantly reduce ice adhesion. For the CYTOP surface, a droplet has a smaller contact area than on untreated substrate but has a larger contact area than the Glaco surface; this can be seen from the surfaces contact angles. Given that the advancing and receding contact angles for CYTOP lie in between that of untreated substrate and Glaco surface, it is reasonable to see the ice adhesion strength to be between those of two surfaces. However, this is not the case for the SOCAL surface as the measured ice adhesion values are much lower than the analytically predicted value. This significant change can be explained with that PDMS chain are flexible and liquid-like on the coated surfaces [15] which has been shown to remain consistent under different environmental conditions. The flexible nature of the PDMS chains means that, as the block has been applied with a horizontal force, the interface between the block and the surface is easily separated, reducing the adhesion of the ice block to the surface. Unlike some other types of PDMS, these chains do not detach locally due to the nature of the strong covalent bonds between the substrate and the chains. Once the block starts moving, the remaining chains which are covered by the block, also move to aid in the removal of the ice and create the effect of a slippery surface. As a combined effect of the low surface energy of the polymeric PDMS chains with a

liquid-like nature, the SOCAL surface exhibits a lower ice adhesion strength than the theory would suggest.

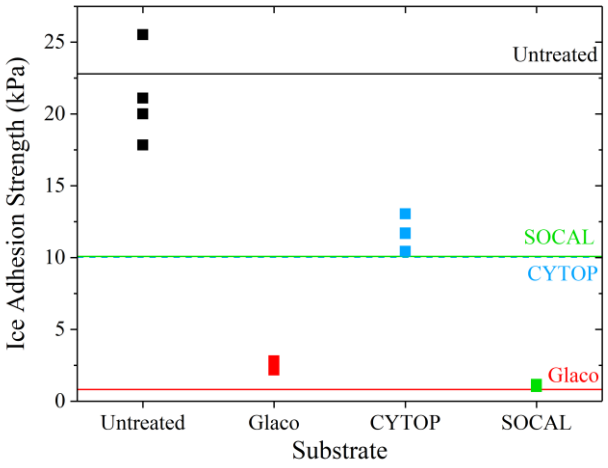

Figure 3) Experimental data for ice adhesion results on cover glass surfaces and compared with analytical values (untreated in black, Glaco in red, CYTOP in light blue dashed and SOCAL in light green solid).

We further investigated the effects of this liquid-like nature of the SOCAL coating for the reduction of ice adhesion on roughened surfaces. The obtained values of adhesion as a function of θ_{rec} for all glass and silicon samples are plotted in Figure 4. The results in Figure 4 are fitted using Equation 1, adjusted using a scaling factor A. All the experimental results are shown to fit using the analytically obtained values, except for the glass SOCAL surface. The ice adhesion data for Si P1200 is larger than Si P120, smooth untreated silicon and cover glass (25.04, 26.85 and 25.67 kPa respectively). This is due to its significantly increased ice contact area arising from the large surface roughness (Table 1) from the introduction of many micro-scale scratches and θ_{rec} (Figure 2a). The large amount of surface features provides strong mechanical interlocking between the ice block and the substrate resulting in larger force required to remove the ice block. For the Si P120 surface, there are fewer but larger surface features. When the ice block is being removed from smooth surfaces, there is the same frictional force required to move across the entire surface. For the Si P120 surface, there are several ridges and valleys, once the ice is dislodged from a ridge, a valley can act as an air pocket which reduces the friction for the ice to move, therefore less force is required. The presence of air pockets from the valleys acts as breaking positions in the mechanical interlocking of the ice block with the surface.

In case of the SOCAL surfaces, the presence of such chains decreases the ice adhesion on all types of silicon samples, including ones with the increased surface roughness. The PDMS chains break the mechanical interlocking between the ice and the surface which, given their flexible nature, therefore reduces the force required to move the ice. Once this interlock has been broken and the first chains start to move, the rest will follow therefore reducing the ice adhesion. Given that the silicon has an ultra-smooth surface compared with the glass surface, when the surface is coated, it requires more force to break the mechanical interlock and move the ice. For the Si P120 SOCAL surface and the Si P1200 SOCAL surface, the adhesion values are 12.84 and 21.05 kPa, respectively. This difference in the ice adhesion strength is arising from differences in the surface roughness, which can also be illustrated through differences in θ_{rec} and $\Delta\theta$ as shown in Figure 2. The Si P120 SOCAL surface has a lower RMS roughness and as such a higher receding angle than Si P1200 SOCAL. The higher receding angle then translates into a lower analytically predicted ice adhesion strength, and this is shown in the experimental data (Figure 4).

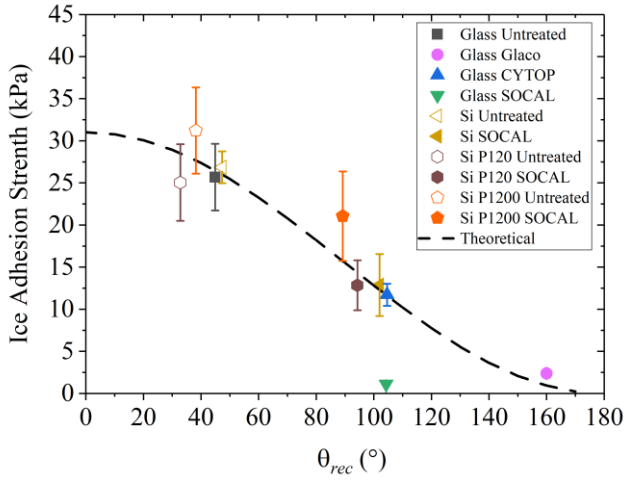

Figure 4) Ice adhesion strength plotted against the theoretical equation for given receding angles.

In this work, we have investigated the effects of wettability on a given substrate to reduce ice adhesion strength of glazed ice. This investigation of reduction in ice adhesion has been realised through the fabrication of three different nanostructure and nanoscale coatings. We have shown that the ice adhesion of a droplet can be reduced to less than 12 kPa using a fluoropolymer coating. We then further reduce the ice adhesion using a nanoparticle coating which reduces ice adhesion to less than 3 kPa. We demonstrate that with the use of a nanoscale SOCAL coating, we can greatly reduce the ice adhesion strength to the magnitude of ~1 kPa. We then compare these results to standard ice adhesion equations, and report that the results match closely with the analytical results. We experimentally investigate the influences of macro and micro scale roughness on the selected SOCAL surface. These results show that for both macro and

micro roughness, the PDMS chain structure present in SOCAL significantly reduces the ice adhesion strength. Furthermore, we report that even with the presence of a macro or microscale substrate roughness, the presence of PDMS chains on the surface lowers the ice adhesion values. The robustness of the wetting properties of all the coatings has also been explored through repeated contact angle and comparisons of contact angle hysteresis after repeated ice adhesion tests comprising of approximately 15 icing/de-icing cycles.

Acknowledgement

This work was supported by the Engineering and Physical Sciences Research Council of UK (EPSRC EP/P018998/1), UK Fluids Network Special Interest Group of Acoustofluidics (EP/N032861/1), EPSRC Centre for Doctoral Training in Renewable Energy Northeast Universities (ReNU) for funding through grant EP/S023836/1.

Conflict of interest

None.

Data availability

The data that support the findings of this study are available from the corresponding author upon reasonable request.

References

1. Frohboese, P. and A. Anders, *Effects of Icing on Wind Turbine Fatigue Loads.* Journal of Physics: Conference Series, 2007. **75**.
2. Carriveau, R., et al., *Ice Adhesion Issues in Renewable Energy Infrastructure.* Journal of Adhesion Science and Technology, 2012. **26**(4-5): p. 447-461.
3. Dalili, N., A. Edrisy, and R. Carriveau, *A review of surface engineering issues critical to wind turbine performance.* Renewable and Sustainable Energy Reviews, 2009. **13**(2): p. 428-438.
4. Gent, R.W., N.P. Dart, and J.T. Cansdale, *Aircraft Icing.* Philosophical Transactions of the Royal Society of London, 2000. **358**: p. 39.
5. Foundation, A.A.S., *Safety Advisory on Aircraft Icing.* 2008: p. 1-16.
6. Parent, O. and A. Ilinca, *Anti-icing and de-icing techniques for wind turbines: Critical review.* Cold Regions Science and Technology, 2011. **65**(1): p. 88-96.
7. Jung, S., et al., *Are superhydrophobic surfaces best for icephobicity?* Langmuir, 2011. **27**(6): p. 3059-66.
8. Cao, L., et al., *Anti-icing superhydrophobic coatings.* Langmuir, 2009. **25**(21): p. 12444-8.

9. Farhadi, S., M. Farzaneh, and S.A. Kulinich, *Anti-icing performance of superhydrophobic surfaces.* Applied Surface Science, 2011. **257**(14): p. 6264-6269.
10. Maissan, J.F., *Wind Power Development in Sub-Acrtic Conditions with Severe Rime Icing*, in *Circumpolar Climate Change Summit and Exposition*. 2001: Whitehorse Yukon, Canda.
11. Kreder, M.J., et al., *Design of anti-icing surfaces: smooth, textured or slippery?* Nature Reviews Materials, 2016. **1**(1).
12. Peng, J., et al., *Enhanced anti-icing properties of branched PDMS coatings with self-regulated surface patterns.* Science China Technological Sciences, 2020. **63**(6): p. 960-970.
13. Liu, B., et al., *Strategies for anti-icing: low surface energy or liquid-infused?* RSC Advances, 2016. **6**(74): p. 70251-70260.
14. Zhang, S., et al., *Bioinspired Surfaces with Superwettability for Anti-Icing and Ice-Phobic Application: Concept, Mechanism, and Design.* Small, 2017. **13**(48).
15. Zhao, X., et al., *Macroscopic Evidence of the Liquidlike Nature of Nanoscale Polydimethylsiloxane Brushes.* ACS Nano, 2021.
16. Sarma, J., et al., *Sustainable icephobicity on durable quasi-liquid surface.* Chemical Engineering Journal, 2022. **431**.
17. Hao, X., et al., *Self-Lubricative Organic–Inorganic Hybrid Coating with Anti-Icing and Anti-Waxing Performances by Grafting Liquid-Like Polydimethylsiloxane.* Advanced Materials Interfaces, 2022. **9**(18).
18. Li, S., et al., *Vapor Lubrication for Reducing Water and Ice Adhesion on Poly(dimethylsiloxane) Brushes.* Adv Mater, 2022. **34**(34): p. e2203242.
19. Wang, L. and T.J. McCarthy, *Covalently Attached Liquids: Instant Omniphobic Surfaces with Unprecedented Repellency.* Angew Chem Int Ed Engl, 2016. **55**(1): p. 244-8.
20. Geraldi, N.R., et al., *Double-sided slippery liquid-infused porous materials using conformable mesh.* Sci Rep, 2019. **9**(1): p. 13280.
21. Armstrong, S., et al., *Pinning-Free Evaporation of Sessile Droplets of Water from Solid Surfaces.* Langmuir, 2019. **35**(8): p. 2989-2996.
22. Yang, D., et al., *Hydrophobically/oleophilically guarded powder metallurgical structures and liquid impregnation for ice mitigation.* Chemical Engineering Journal, 2022. **446**.

Author photograph and biography

Luke Haworth

Luke Haworth is a postgraduate research student at Northumbria University since September 2020. He obtained a Frist Class (Honours) MPhys also form Northumbria in 2020. His current postgraduate research topic is the study of anti-icing and de-icing using smart coatings and surface acoustic waves.

Deyu Yang

Deyu Yang, a postdoctoral researcher in Northwestern Polytechnical University since February 2023. He obtained his Doctoral degree in Materials Engineering and Materials Design from the University of Nottingham (UK) in 2023. He obtained his MEng in Metallurgical Engineering at the Beijing General Research Institute for Nonferrous Metals (China) in 2018, and his BEng in Metallurgical Engineering at the Central South University (China) in 2015.

Prashant Agrawal

Prashant Agrawal is an assistant professor at Northumbria University. His research interests are in experimental and numerical understanding of soft matter and multiphase fluid dynamics and its applications in healthcare diagnostics, forensics and energy harvesting.

Hamdi Torun

Hamdi Torun is an associate professor at Northumbria University. Previously, he was an associate professor at Bogazici University, Turkey. He is a cofounder of GlakoLens, a biomedical spinoff company. He received Technology Award from Elginkan Foundation, Turkey in 2016, Young Scientist Award from The Science Academy, Turkey in 2016, Innovator Under 35 Award from MIT Tech Review in 2014, and Marie Curie Fellowship (MC-IRG Grant) in 2011. His expertise is in development of integrated micro/nanosystems especially for sensing applications.

Xianghui Hou

Xianghui Hou is a professor at the School of Materials Science and Engineering, Northwestern Polytechnical University, China. He is also a Fellow of the Institute of Materials, Minerals and Mining (FIMMM). His current research interests include icephobic coatings, composites, and nanostructured materials.

Glen McHale

Glen McHale is Professor of Interfacial Science & Engineering at The University of Edinburgh and a member of the Institute for Multiscale Thermofluids. He was previously Pro Vice Chancellor/Executive Dean of the Faculty of Engineering & Environment at Northumbria University, UK. He is a Fellow of the Higher Education Academy (HEA), the Institute of Physics (IoP), the Royal Society for Arts, Manufactures and Commerce (RSA) and is a Senior Member of the Institute of Electrical and Electronics Engineers (SMIEEE). His research focuses on acoustic wave sensors, static and dynamic

wetting, dielectrowetting, liquid friction and superhydrophobic, liquid infused and slippery liquid-like sold surfaces.

Richard Fu

Richard YongQing Fu is a professor in the Faculty of Engineering and Environment, University of Northumbria at Newcastle, UK. He has extensive experience in smart thin films/materials, biomedical microdevices, energy materials, lab-on-chip, micromechanics, MEMS, nanotechnology, sensors and microfluidics. He published over 450 journal papers with Google scholar H-index of 72 and over 22K citations. He is associate editors/editorial board members for seven international journals including *Nanotechnology and Precision Engineering*, and *Scientific Report*.